Numerical tests of RMT in lattice QCD

Urs M. Heller

American Physical Society & BNL

ECT* workshop “RMT in Sub-Atomic Physics and Beyond.”
In honor of Jac Verbaarschot’s 65th birthday.
Trento, Italy

Aug 5–9, 2019

Collaborations

Part of this research was done in collaboration with

- P.H. Damgaard and A. Krasnitz, Phys. Lett. B445 (1999) 366 [arXiv:hep-lat/9810060]
- R.G. Edwards, J. Kiskis and R. Narayanan, Phys. Rev. Lett. 82, 4188 (1999) [arXiv:hep-th/9902117]
- R.G. Edwards and R. Narayanan, Phys. Rev. D60, 077502 (1999) [arXiv:hep-lat/9902021]
- P.H. Damgaard, R. Niclasen and K. Rummukainen, Phys. Rev. D61, 014501 (1999) [arXiv:hep-lat/9907019]
- P.H. Damgaard, R. Niclasen and K. Rummukainen, Phys. Lett. B495 (2000) 263 [arXiv:hep-lat/0007041]
- P.H. Damgaard and K. Splittorff, Phys. Rev. D85, 014505 (2012) [arXiv:1110.2851]
- P.H. Damgaard and K. Splittorff, Phys. Rev. D86, 094502 (2012) [arXiv:1206.4786]

See also: UMH, PoS Lattice 2011 (2011) 103 [arXiv:arXiv:1112.1914]

Introduction

Random matrix theory was introduced for the description of low energy properties of QCD, in particular for the finite volume Dirac operator spectrum, by Jac and collaborators:

E.V. Shuriak and J.J.M. Verbaarschot, Nucl. Phys. A560 (1993) 306 [arXiv:hep-th/9212088];
J.J.M. Verbaarschot and E. Zahed, Phys. Rev. Lett. 70, 3852 (1994) [arXiv:hep-th/9303012];
J.J.M. Verbaarschot, Phys. Lett. B329 (1994) 350 [arXiv:hep-th/9402008]; Nucl. Phys. B426 (1994) 559 [arXiv:hep-th/9401092]; Phys. Rev. Lett. 72, 2531 (1994) [arXiv:hep-th/9401059].

Gauge theories with various gauge groups and fermions in different representation fall into three different universality classes of spontaneous chiral symmetry breaking and corresponding classes of RMT ensembles.

- Pseudo-real rep.: enhanced to $SU(2N_f) \to Sp(2N_f)$; chOE
- Complex rep.: $SU(N_f) \times SU(N_f) \to SU(N_f)$; chUE
- Real rep.: enhanced to $SU(2N_f) \to SO(2N_f)$; chSE

See also P.H. Damgaard, UMH, R. Niclasen and B. Svetitsky, Nucl. Phys. B633 (2002) 97 [arXiv:hep-lat/0110028]

Microscopic spectral density

The rescaled, with the condensate $\Sigma = \pi\rho(0)$, microscopic spectral density,

$$\rho_s(\zeta) = \frac{1}{V}\rho\left(\frac{\zeta}{V\Sigma}\right) ; \qquad \zeta = \lambda V \Sigma \, ,$$

is universal. For the chiral unitary ensemble it is given by,

$$\rho_s(\zeta) = \pi\rho(0)\frac{\zeta}{2}\left[J_{N_f+\nu}(\zeta)^2 - J_{N_f+\nu+1}(\zeta)J_{N_f+\nu-1}(\zeta)\right] \, .$$

Here ν is the fixed index, or the fixed topological charge, of the sector considered, V the finite volume, and N_f the number of dynamical fermion flavors.

G. Akemann, P.H. Damgaard, U. Magnea and S.M. Nishigaki, Nucl. Phys. B487 (1997) 721 [arXiv:hep-th/9609174];
P.H. Damgaard and S. Nishigaki, Nucl. Phys. B518 (1998) 495 [arXiv:hep-th/9711023];

Smallest eigenvalue distributions

Also universal, with known analytic expressions, are the distributions of the lowest rescaled eigenvalue. For the $N_f = 0$ unitary ensemble one finds, *e.g.*,

$$P_{\min}(\zeta) = \begin{cases} \frac{\zeta}{2} \mathrm{e}^{-\zeta^2/4} & \text{if } \nu = 0\,, \\ \frac{\zeta}{2} I_2(\zeta) \mathrm{e}^{-\zeta^2/4} & \text{if } \nu = 1\,. \end{cases}$$

P.J. Forrester, Nucl. Phys. B402 (1993) 709;
S.M. Nishigaki, P.H. Damgaard and T. Wettig, Phys. Rev. D58, 087704 (1998) [arXiv:hep-th/9803007].

Further, it can be shown that the eigenvalue distributions can be obtained directly from the finite volume partition function of QCD, that is from the zero-momentum part of the chiral Langrangian, without resorting to RMT.

P.H. Damgaard, Phys. Lett. B424 (1998) 322 [arXiv:hep-th//9711047];
G. Akemann and P.H. Damgaard, Nucl. Phys. B528 (1998) 411 [arXiv:hep-th/9801133]; Phys. Lett. B432 (1998) 390 [arXiv:hep-th/9802174];
J. Osborn, D. Toublan and J.J.M. Verbaarschot, Nucl. Phys. B540 (1999) 317 [arXiv:hep-th/9806110].

First tests with staggered fermions

The first numerical tests for 4d QCD-like theories were performed with staggered fermions for gauge group SU(2), both in the quenched approximation, $N_f = 0$, and with dynamical fermions.

For staggered fermions, with the Dirac matrices replaced by real-valued phases, however, the chiral symmetry breaking patterns, and thus RMT ensembles, are changed compared to continuum fermions.

- Pseudo-real rep.: chSE
- Complex rep.: chUE
- Real rep.: chOE

chSE and chOE are interchanged!

Examples for gauge group and fermion representation for each of the three cases are:

- Pseudo-real rep.: SU(2) fundamental representation
- Complex rep.: SU(3) fundamental representation
- Real rep.: SU(N) adjoint representation

Staggered fermions: SU(2) fundamental

The quenched microsopic spectral density and distribution of the smallest eigenvalue, compared with chSE predictions:

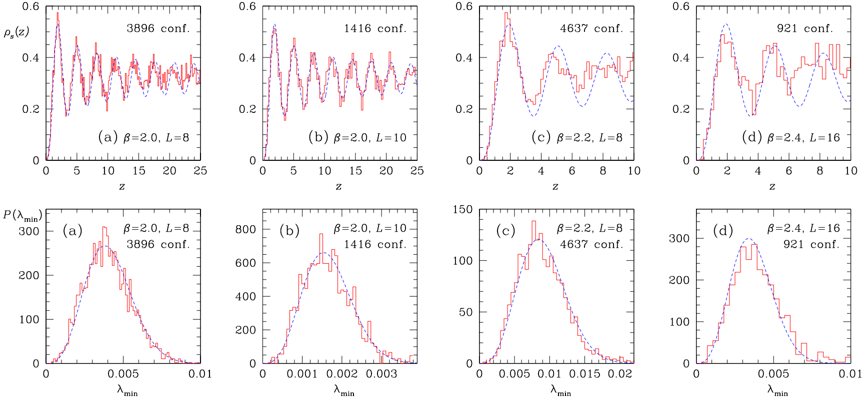

M.E. Berbenni-Bitsch, S. Meyer, A. Schäfer, J.J.M. Verbaarschott and T. Wettig, Phys. Rev. Lett. 80, 1146 (1998) [arXiv:hep-lat/9704018];

Staggered fermions: SU(2) fundamental

The distribution of the smallest eigenvalue and microsopic spectral density for a dynamical ensemble with one staggered flavor. $\mu = mV\Sigma$ is the rescaled mass of the dynamical fermions. Because of a global charge conjugation symmetry, the comparison is to RMT with $N_f = 2$.

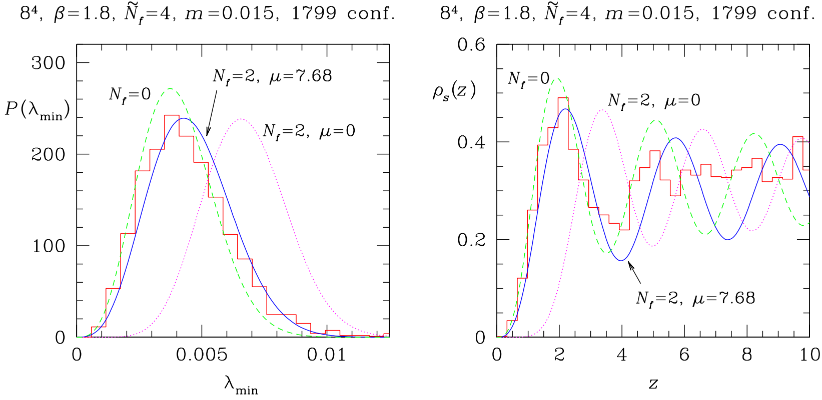

M.E. Berbenni-Bitsch, S. Meyer and T. Wettig, Phys. Rev. D58, 071502 (1998) [arXiv:hep-lat/9804030].

Staggered fermions: SU(3) fundamental

For SU(3) fermions in the fund. rep., chUE, we (PHD, UMH, AK) find:

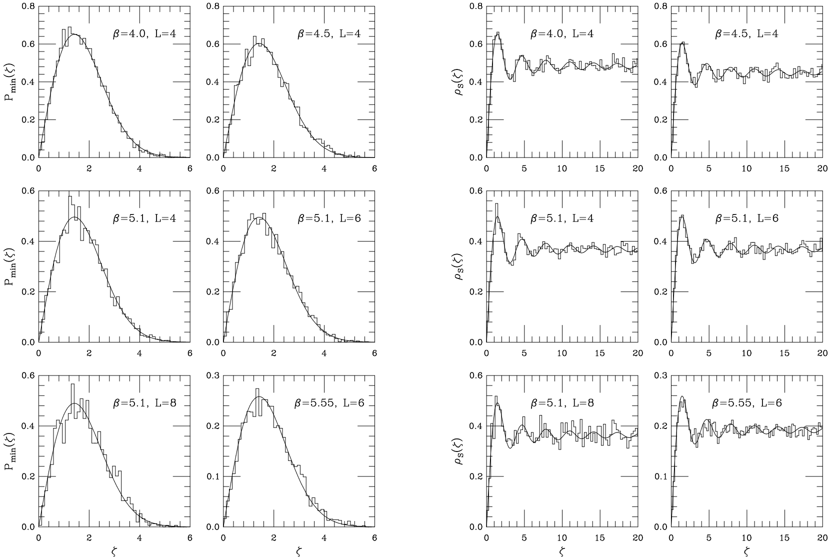

Staggered fermions: SU(2) and SU(3) adjoint

For SU(N), $N = 2,\ 3$, fermions in the adjoint rep., chOE, we (RGE, UMH, RN) find:

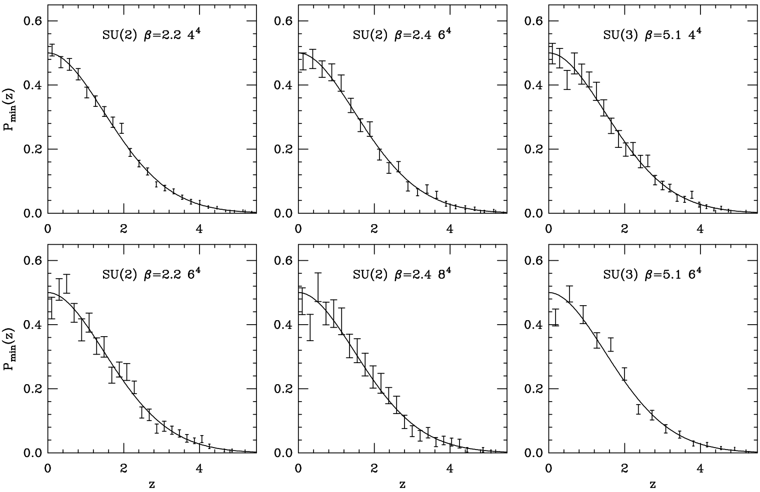

Staggered fermions: SU(2) and SU(3) adjoint

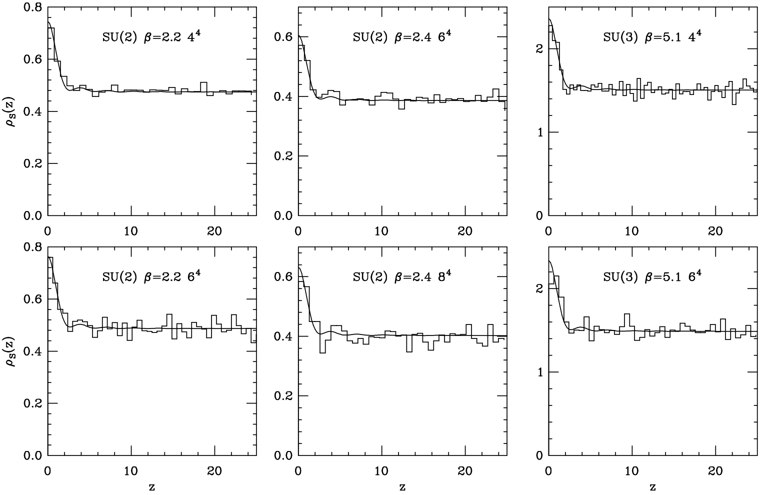

Staggered fermions: SU(3) fund, 10 evs

Integral expressions have been derived for *k*-th eigenvalue distributions.

P.H. Damgaard and S.M. Nishigaki, Phys.Rev. D63, 045012 (2001) [arXiv:hep-th/0006111].

We (PHD, UMH, RN, KR) compared with quenched staggered results:

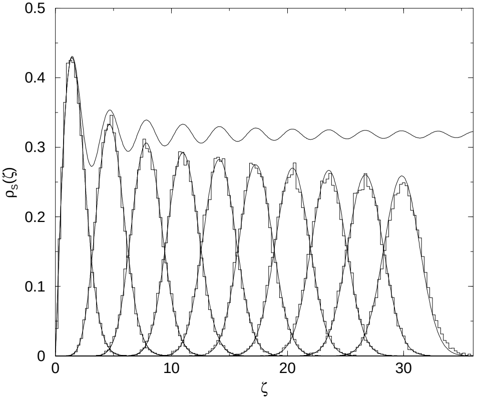

Staggered fermions: one flavor dynamical

We (PHD, UMH, RN, KR) also compared with $N_f = 1$, *i.e.*, one staggered dynamical flavor, results. $\mu = mV\Sigma$ is again the rescaled mass of the dynamical fermions.

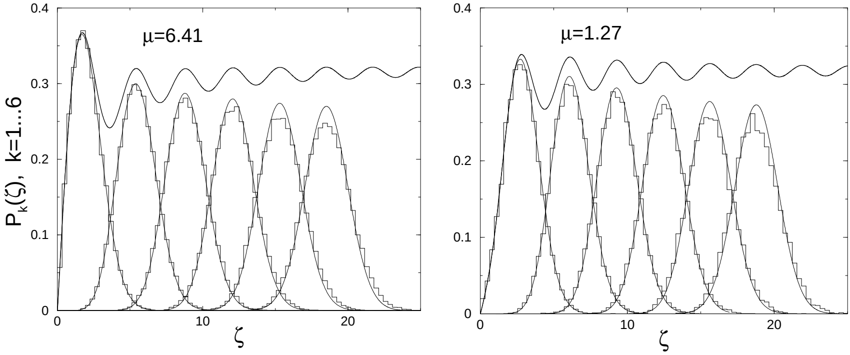

Staggered fermions: one flavor dynamical

We also checked the mass dependence of the RMT prediction, here for the miscroscopic spectral density.

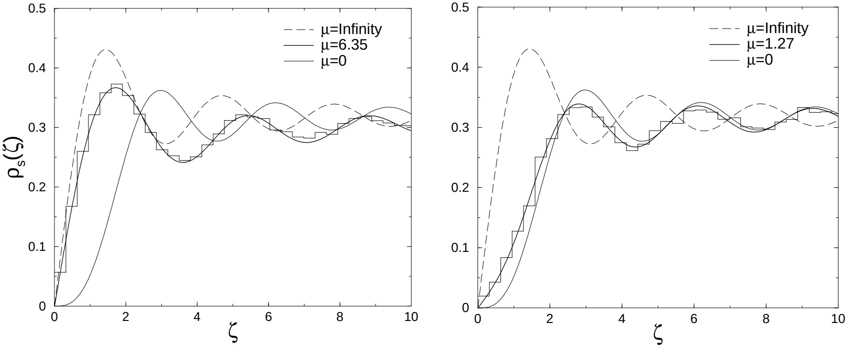

Staggered fermions and topology

At the strong couplings and hence large lattice spacings used so far, the staggered lattice effects are so large that the eigenvalues do not come in quadruplets, for the $N_t = 4$ continuum fermions, but are equally spaced.

Even at a smaller lattice spacing, $a \approx 0.09$ fm, only highly improved staggered fermions start showing the quarduplet structure.

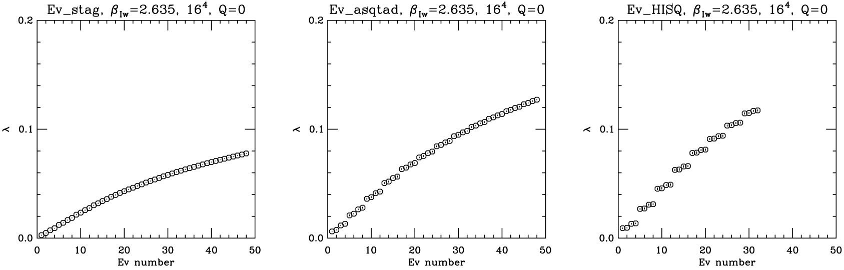

Staggered fermions and topology

And only with highly improved staggered fermions do the "almost" zeromodes in topologically nontrivial sectors start to emerge.

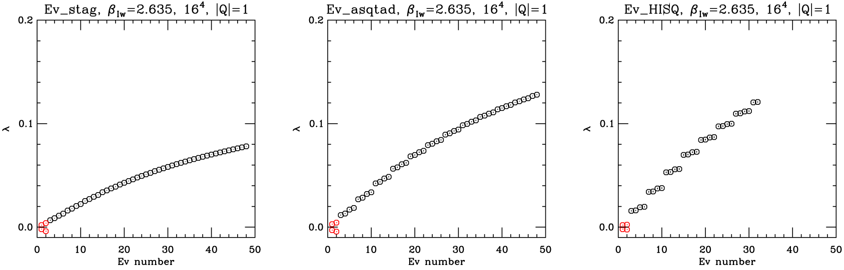

For the large lattice spacing used to compare with RMT predictions, we (PHD, UMH, RN, KR) found the the staggered results agree with the $\nu = 0$ RMT predictions, used for all previous comparions, regardless of the topological charge sector, determined with cooling and a gauge field definition of the topological charge.

Staggered fermions: insensitive to topology

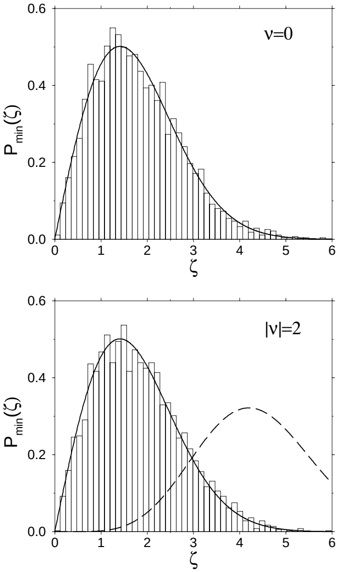

Staggered fermions: insensitive to topology

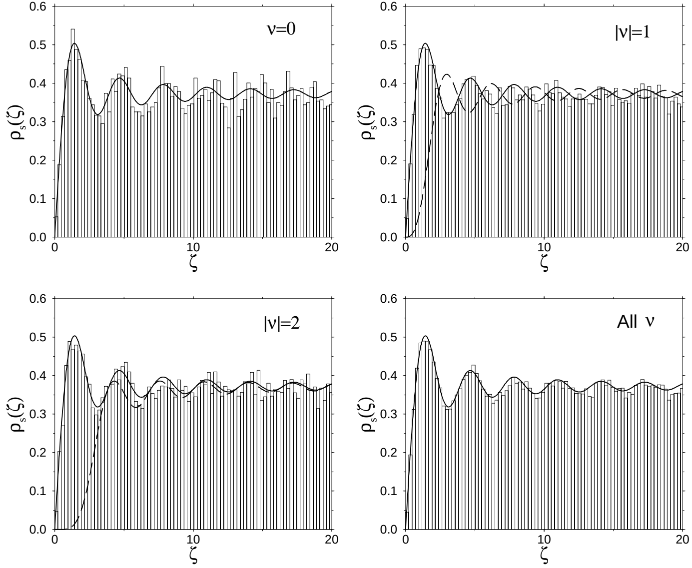

First tests with overlap fermions

The tests with staggered fermions presented so far have two drawbacks:

- Two of the universality classes, chOE and chSE, are interchanged with respect to continuum fermions.
- At the (large) lattice spacing used, staggered fermions are insensitive to the topological charge and so only $\nu = 0$ predictions have been tested.

Overlap fermions overcome both these drawbacks. They have the same chiral symmetries as continuum fermions and they are sensitive to topology, having exact zeromodes in topologically nontrivial sectors.

R. Narayanan and H. Neuberger, Nucl. Phys. B443 (1995) 305 [arXiv:hep-th/9411108];
H. Neuberger, Phys. Lett. B417 (1998) 141 [arXiv:hep-lat/9707022].

We (RGE, UMH, JK, RN) considered an example from each of the three RMT universality classes both in the sector with $\nu = 0$ and $\nu = 1$, where we, of course, also found an exact zeromode.

First tests with overlap fermions

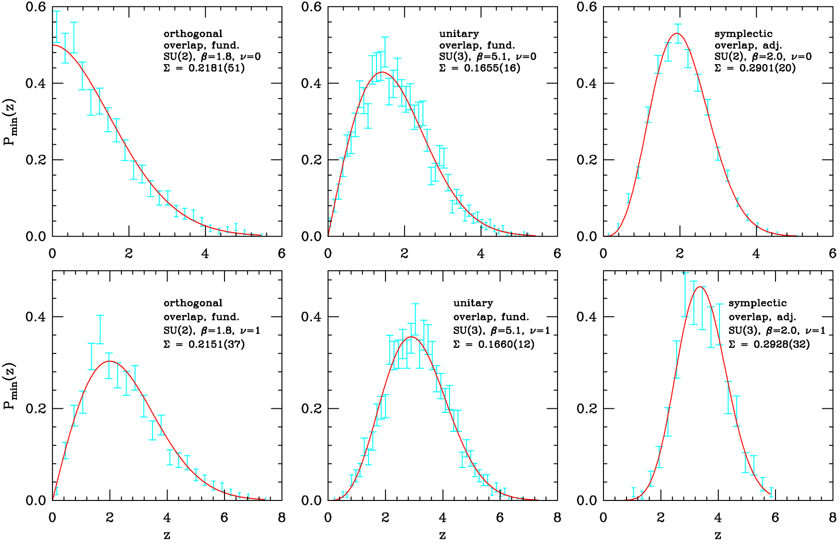

Including staggered lattice effects

At low energy, the leading fermion discretization effects can be included in χPT by considering a modified chiral Langrangian

$$\mathcal{L} = \frac{f^2}{8} \mathrm{Tr}\left(\partial_\mu U \partial_\mu U^\dagger\right) - \frac{1}{2} m \Sigma \mathrm{Tr}\left(U + U^\dagger\right) + a^2 \mathcal{V} \ .$$

$\mathcal{V}$ describes the taste breaking terms

$$\mathcal{V} = -\frac{1}{2} C_4 \mathrm{Tr}\left(\xi_{\mu 5} U \xi_{5\mu} U^\dagger + h.c.\right) + \dots \ ,$$

where we only displayed the numerically dominant term (for pseudoscalar mass splittings) explicitly. Here $\xi_\mu = \gamma_\mu^*$ are taste matrices.

In the ϵ-regime of χPT the zero momentum modes dominate and the first term in $\mathcal{L}$ can be neglected. The ϵ-regime can equivalently be discribed by chiral RMT, with the Dirac operator represented as

$$\mathcal{D} = \mathcal{D}_0 \otimes \mathbb{I}_4 + a\mathcal{T} \ ,$$

Including staggered lattice effects

$$\mathcal{D}_0 = \begin{pmatrix} 0 & iW \\ iW^\dagger & 0 \end{pmatrix}$$

with W a random $(N+\nu) \times N$ complex matrix.

$\mathcal{T}$ denotes taste-breaking terms with the dominant one taking the form

$$\mathcal{T}_{C_4} = \begin{pmatrix} A_\mu & 0 \\ 0 & B_\mu \end{pmatrix} \otimes \xi_{\mu 5}$$

with A_μ and B_μ Gaussian random Hermitian matrices of size $(N+\nu) \times (N+\nu)$ and $N \times N$, respectively, with width proportinal to C_4.

The dimensionless combination $a^2 C_4 V$ controls the strength of the taste breaking in staggered RMT. For weak taste breaking, $a^2 C_4 V \ll 1$, the quartets of eigenvalues are split at leading order into pairs, which are slightly split at second order. The splittings are

$$\frac{\Delta\lambda_2}{\lambda} \propto a\sqrt{C_4 V}\,, \qquad \frac{\Delta\lambda_1}{\lambda} \sim \frac{\Delta\lambda_3}{\lambda} \propto a^2 C_4 V\,.$$

For more details, see

J. Osborn, Phys. Rev. D83, 034505 (2011) [arXiv:1012.4837].

Including staggered lattice effects

We compare distributions of eigenvalues from ~ 1200 $Q = 0$, $a = 0.093$ fm, and $L = 1.5$ fm configurations with MC generated staggered RMT $\nu = 0$ eigenvalue distributions.

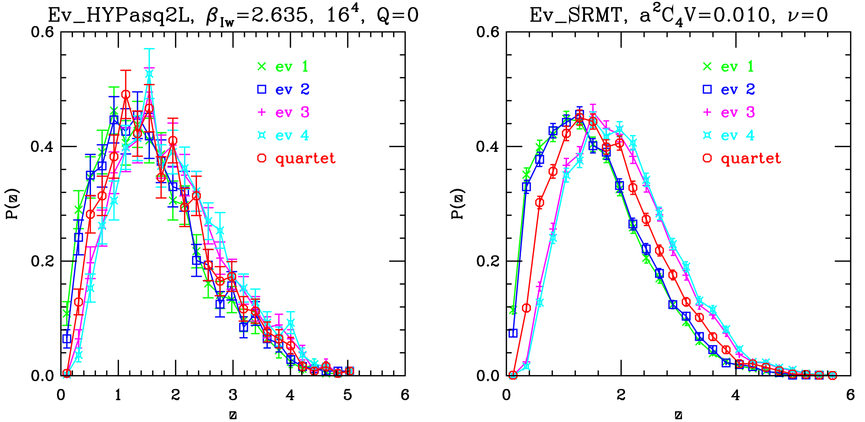

Qualitatively, the distributions look quite similar.

Including staggered lattice effects

The same for ~ 2000 $|Q| = 1$ configurations and $\nu = 1$ staggered RMT MC generated eigenvalue distributions.

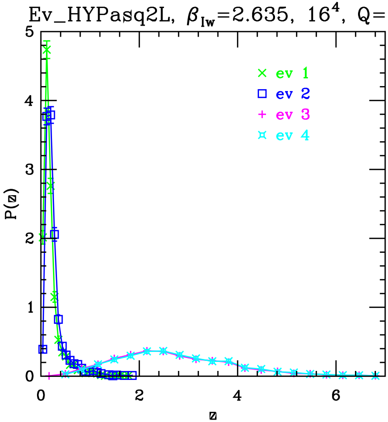

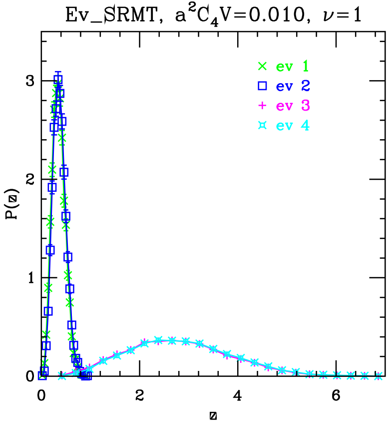

The slightly lower peak for the "would-be zeromodes" on the right indicates that the value of $a^2 C_4 V$ used is a little too large.

Including lattice effects for Wilson fermions

In the ϵ-regime, and with the power counting $m \sim a^2$, the zero momentum part of the Wilson chiral Lagrangian is

$$\mathcal{L} = -\frac{1}{2} m\Sigma \mathrm{Tr}\left(U + U^\dagger\right) + a^2 W_8 \mathrm{Tr}\left(U^2 + U^{\dagger 2}\right) + a^2 W_6 \left[\mathrm{Tr}\left(U + U^\dagger\right)\right]^2 + a^2 W_7 \left[\mathrm{Tr}\left(U - U^\dagger\right)\right]^2 .$$

The two-trace terms of the second line are suppressed at large N_c.

The Dirac operator for the chiral RMT including the one-trace term is

$$\mathcal{D}_W = \begin{pmatrix} \tilde{a}A & iW \\ iW^\dagger & \tilde{a}B \end{pmatrix}$$

with W a random $(N+\nu)\times N$ complex matrix, and A and B random Hermitian matrices of size $(N+\nu)\times(N+\nu)$ and $N \times N$, respectively. $\mathcal{H}_W = \gamma_5\left(\mathcal{D}_W + \tilde{m}\right)$ is the RMT equivalent of Hermitian Wilson Dirac operator $H_W = \gamma_5\left(D_W + m\right)$ with

$$\hat{m} = m\Sigma V = 2\tilde{m}N \quad \text{and} \quad \hat{a}^2 = \hat{a}_8 = a^2 W_8 V = \frac{1}{2}\tilde{a}^2 N$$

held fixed. The rescaling is with ΣV for QCD or $2N$ in RMT.

Including lattice effects for Wilson fermions

G. Akemann, P.H. Damgaard, K. Splittorff, J.J.M. Verbaarschot, Phys. Rev. D83 085014 (2011) [arXiv:1012.0752] have worked out the eigenvalue distribution of the Hermitian Wilson Dirac operator in Wilson χPT and G. Akemann and T. Nagao, JHEP 10 (2011) 060 [arXiv:1108.3035] reproduced the results directly from Wilson RMT.

The two-trace terms can be incorporated via two Gaussian integrations

$$Z^\nu(\hat{m}, \hat{z}; \hat{a}_6, \hat{a}_7, \hat{a}_8) = \frac{1}{16\pi \hat{a}_6 \hat{a}_7} \int_{-\infty}^{\infty} dy_6 dy_7 \mathrm{e}^{-\frac{y_6^2}{16\hat{a}_6^2} - \frac{y_7^2}{16\hat{a}_7^2}} Z^\nu(\hat{m} - y_6, \hat{z} - y_7; 0, 0, \hat{a}_8) \,,$$

where $Z^\nu(\hat{m}, \hat{z}; 0, 0, \hat{a}_8)$ is the fixed-index partition function including the one-trace $\mathcal{O}(a^2)$ term and with a $\bar{\psi}\gamma_5\psi$ term represented in the chiral Langrangian as $\Delta\mathcal{L} = -\frac{1}{2} z\Sigma \mathrm{Tr}\left(U - U^\dagger\right)$ and $\hat{z} = z\Sigma V$.

Including lattice effects for Wilson fermions

For our (PHD, UMH, KS) test in the quenched case, we generated three ensembles using the Iwasaki gauge action, which suppresses dislocations, and gives a fairly unique index (topol. charge Q).

β_{Iw}	r_0/a	a [fm]	size	L [fm]	cfgs	$\nu = 0, 1, -1$
2.635	5.37	0.093	16^4	1.5	6500	1246, 1088, 1045
2.635	5.37	0.093	20^4	1.9	3000	379, 319, 322
2.79	6.70	0.075	20^4	1.5	6000	1172, 990, 988

I first show results from the comparison of the lowest (in magnitude) 20 eigenvalues of the Hermitian Wilson Dirac operator, with 1 HYP smearing, for bare mass $am_0 = -0.216$ on the the 16^4 ensemble with $a = 0.093$ fm, $L = 1.5$ fm) with Wilson RMT.

The strategy was to find values for the Wilson RMT parameters $\hat{a}$ and $\hat{m}$, and the eigenvalue rescalig factor ΣV so that Wilson RMT "fits" the measured (histogrammed) distribution "well" (by eye) for $Q = 0$. Using the same parameter values, Wilson RMT then predicts the $|Q| = 1$ distribution that can be compared with the measured one.

Including lattice effects for Wilson fermions

Testing Wilson RMT for for $Q = 0$ (left) to determine Wilson RMT paramenters and for $|Q| = 1$ (right) which follows as a prediction.

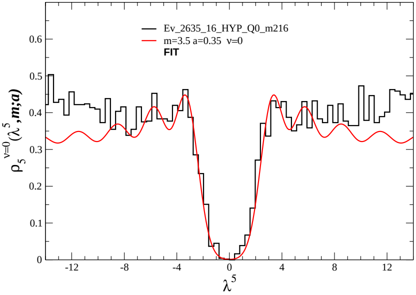

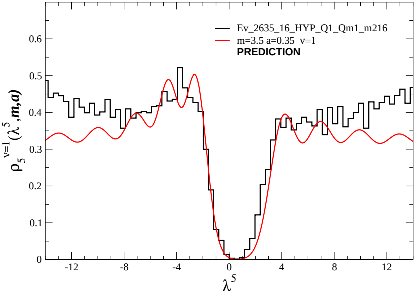

Wilson RMT describes the data quite well!

Including lattice effects for Wilson fermions

Using volume scaling, $\hat{a}_B = \hat{a}_A\sqrt{V_B/V_A}$ and $\hat{m}_B = \hat{m}_A(V_B/V_A)$ we get predictions for both the $Q = 0$ and $|Q| = 1$ sectors on the larger volume at otherwise the same parameters.

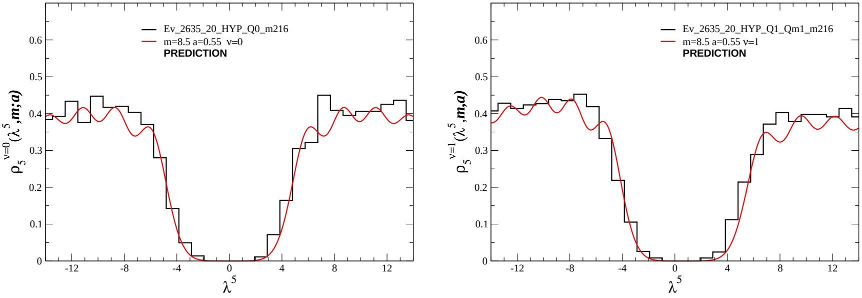

Again Wilson RMT describes the data quite well!

Including lattice effects for Wilson fermions

Next, on the fines lattice ensemble, we tested the mass dependence of Wilson RMT predictions. We first considered bare mass $am_0 = -0.184$ and determined the Wilson RMT in the $Q = 0$ sector (left) and used them for predicitions in the $|Q| = 1$ sector (right).

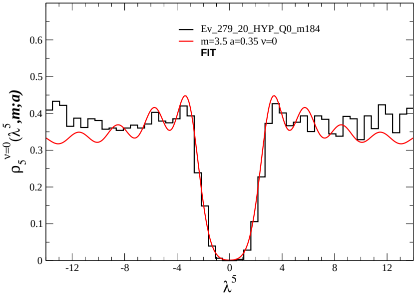

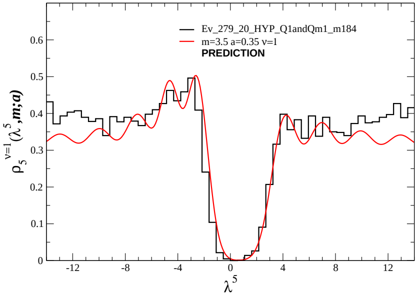

Again Wilson RMT describes the data quite well!

Including lattice effects for Wilson fermions

Next, we considered bare mass $am_0 = -0.178$ and compared with Wilson RMT with the mass parameter rescaled by $\Delta\hat{m} = \Delta m_0 \Sigma V$.

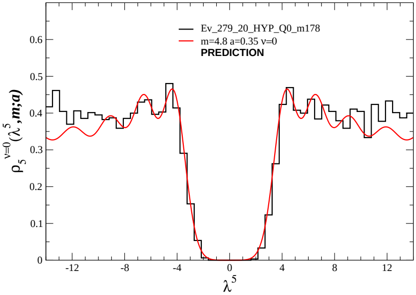

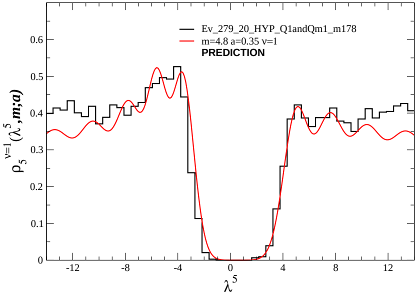

For both $Q = 0$ and $|Q| = 1$ Wilson RMT predicts the data quite well!

Including lattice effects for clover fermions

On the same configurations, we also considered clover improved fermions, again with 1 HYP smearing and clover coefficient set to 1. We show examples from the coarser lattice for $Q = 0$ (left) and $|Q| = 1$ (right).

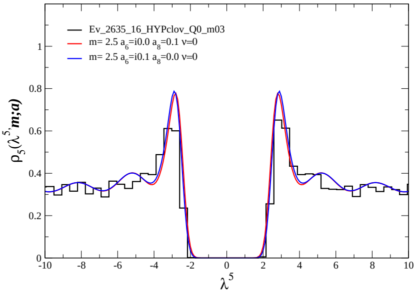

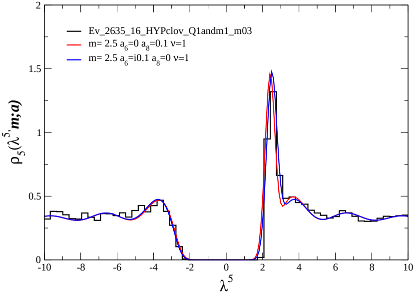

Wilson RMT describes the data quite well, with lattice effects about a factor 3-4 reduced from Wilson fermions. This leads, in particular, to the higher peak from the "zero modes" for $|Q| = 1$.

We can describe the data equally well with either $\hat{a}_8$ or $\hat{a}_6$ nonzero.

Including lattice effects for clover fermions

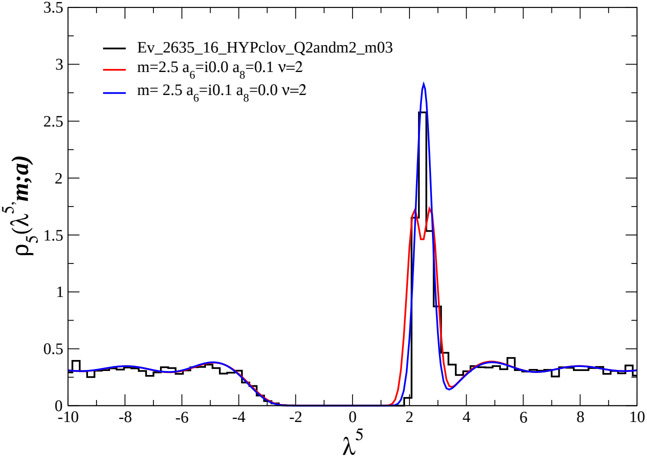

The $|Q| = 2$ sector, however, stongly favors $\hat{a}_6 \neq 0$. $\hat{a}_8 \neq 0$ would lead to level repulsion among the two "zero modes" that we do not observe.

Conclusions

I have reviewed numerical tests of RMT predictions in (lattice) QCD.

- We have completed the test for all RMT ensembles with staggered fermions, chUE, SU(3) fund., and chOE, SU(N) adjoint; chSE, SU(2) fund., had been done before.
- The drawbacks of staggered fermions are
  - chOE and chSE are interchanged compared to continuum fermions;
  - At the large lattice spacings used, staggered fermions are insensitive to topology, so only the $\nu = 0$ predictions could be tested.
- Overlap fermions overcome both these drawbacks and we performed test for all three RMT ensembles in topological sectors with $\nu = 0$ and $\nu \neq 0$.
- Finally we performed tests of extensions of RMT to include lattice artefacts both for staggered and Wilson fermions.

All these tests were sucessful!

Happy birthday, Jac!